

Evaluating the Effect of Tomosynthesis Acquisition Parameters on Image Texture: A Study Based on an Anthropomorphic Breast Tissue Software Model

Despina Kontos¹, Cuiping Zhang¹, Nicole Ruitter², Predrag R. Bakic¹,
and Andrew D.A. Maidment¹

¹University of Pennsylvania, Department of Radiology, Physics Section, 1 Silverstein Building
HUP, 3400 Spruce St., Philadelphia PA 19104-4206

{Despina.Kontos, Cuiping.Zhang, Predrag.Bakic,
Andrew.Maidment}@uphs.upenn.edu

²Forschungszentrum Karlsruhe, Karlsruhe, Germany
Nicole.Ruitter@ipe.fzk.de

Abstract. Mammographic texture features have been shown to correlate with the risk of developing breast cancer. Digital breast tomosynthesis (DBT) is an emerging 3D x-ray breast imaging modality with superior tissue visualization compared to mammography, having the potential to provide more accurate estimation of parenchymal texture features. In this paper, we investigate the effect of DBT acquisition parameters on computer-extracted texture features. DBT images were simulated using an anthropomorphic breast tissue software model allowing for variations in DBT acquisition geometry. Our results show that DBT acquisition geometry appears to have an impact on the computed texture features; angular range appears to have a greater effect than the selected number of source projections. We attribute this effect to the differences in image quality resulting from the different reconstruction geometries. Our ultimate goal is to determine the DBT acquisition geometry that provides the optimal image quality to estimate parenchymal texture.

Keywords. Digital breast tomosynthesis, acquisition geometry, parenchymal texture analysis, breast tissue software model.

1 Introduction

Growing evidence suggests that mammographic parenchymal patterns are indicative of the risk of developing breast cancer [1]. While the relationship between mammographic breast density and breast cancer risk has been clearly demonstrated [1], studies have also shown a potential association between mammographic parenchymal texture and breast cancer risk [2]. Computerized analysis of digitized mammograms has shown the potential to distinguish the parenchymal patterns of BRCA1/2 gene mutation carriers using parenchymal texture features from the retroareolar breast region [2]. These studies suggest that computer-extracted texture features, could provide alternative, fully-automated, and reproducible methods to characterize parenchymal patterns for breast cancer risk estimation.

Digital breast tomosynthesis (DBT) is an emerging x-ray imaging modality in which tomographic images of the breast are reconstructed from multiple low-dose x-ray source projections acquired at different angles of the x-ray tube [3]. Having the advantage of tomographic imaging, DBT alleviates the effect of tissue superimposition and offers superior tissue visualization compared to conventional mammography. Early clinical trials have shown that DBT could result in higher sensitivity and specificity compared to mammography [3]. Our preliminary studies also suggest that DBT parenchymal texture analysis could outperform mammography in breast cancer risk estimation [4, 5].

As DBT is currently a device under investigation, several manufactures are evaluating different DBT prototypes systems, considering a range of different acquisition geometries and reconstruction algorithms, to achieve optimal image quality for clinical applications. Previously, Maidment *et al.* have shown, analytically and through simulations, that both the use of more source projection images and the use of a larger angular range for the x-ray tube rotation improve DBT image quality [6]. Here, we investigate the extent in which DBT acquisition geometry affects the estimation of parenchymal texture features. Our ultimate goal is to determine the DBT reconstruction geometry that provides the optimum image quality for estimating parenchymal texture features, and therefore provide the most accurate measures for breast cancer risk estimation.

2 Methods

DBT simulation was performed using an anthropomorphic breast tissue software model, previously developed in our lab for generating synthetic mammograms [7]. The model allows for variations in breast volume, breast composition, compression force, and acquisition geometry. Recently, we augmented the model to include a region growing procedure in order to produce more realistic synthetic x-ray breast images [8], and also consider finite element simulation of the breast deformation to account for clinical breast compression [9]. For DBT simulation, a simple ray-tracing

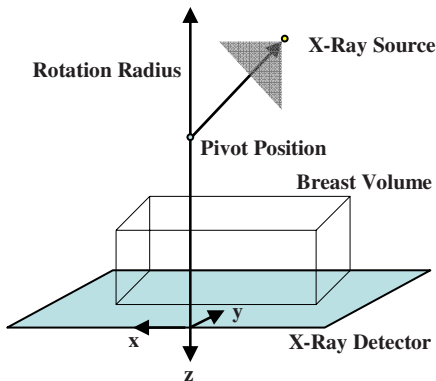


Fig. 1. Simulation of DBT geometry

model is used to simulate a variety of acquisition geometries [9]. The x-ray source is assumed to be a point source emitting monoenergetic primary radiation (Fig. 1).

The DBT acquisition geometry parameters can be varied to allow simulation of different setups. In this study, the DBT geometry was chosen to match our clinical setting (Senographe DS, GE, Milwaukee, WI). The detector dimensions were equal to 230.4 mm x 192 mm, with 0.1 mm² detector elements. The x-ray beam energy was set at 20 keV. The linear x-ray attenuation coefficients were set

to $\mu_1=0.456 \text{ cm}^{-1}$ for adipose tissue and $\mu_2= 0.802 \text{ cm}^{-1}$ for glandular, connective, and skin tissues.

For our analysis, a 700ml breast volume was simulated with 30% tissue glandularity (*i.e.* breast percent density). This volume corresponds to an average middle-range (*i.e.* Cup C) breast. Breast thickness was reduced by 20%, using finite element simulation of breast deformation to account for the relatively lower compression force commonly used in DBT. To evaluate the effect of DBT geometry on texture, twelve different DBT geometries were used to generate projection images, differing by the angular range of the x-ray tube rotation and number of simulated source projection images. The total angular range of the x-ray tube rotation was defined as 20° , 30° or 40° , discretized in 7, 9, 11, or 15 equiangular steps. Filtered-backprojection was used to reconstruct twelve synthetic DBT volumes, with 80 tomographic planes at 1mm increments with 0.22mm in-plane resolution (Fig. 2.a).

Retroareolar (2.5 cm^3) regions of interest (ROIs) were manually segmented from all the synthetic DBT images (Fig. 2.b). Texture features of skewness, coarseness, contrast, and energy were estimated. These features have been shown in previous studies with mammograms to correlate with the risk of developing breast cancer [2]. For each texture descriptor, a feature f_i , $i=1 \dots T$ was computed from each tomographic plane of the 3D DBT ROIs ($T=26$ slices, 1mm/slice).

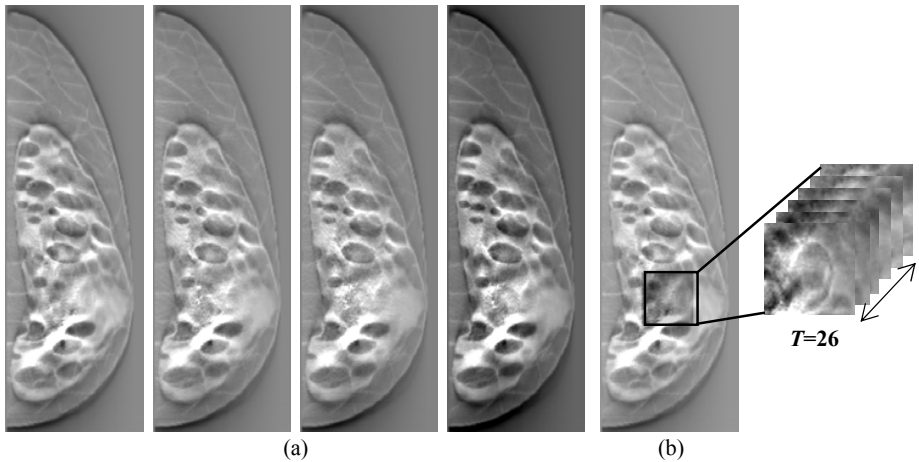


Fig. 2. Slices of the simulated DBT images. (a) Left to right: central slice reconstructed from 20° angular range and 9 projections, $30^\circ/9$, $40^\circ/9$, and $40^\circ/15$. (b) Example of a retroareolar ROI.

Skewness reflects the properties of the gray-level histogram and has been used to assess parenchymal density [2]. When the image texture is predominantly composed of fat (*i.e.* the grey-level histogram is skewed to higher values) the skewness tends to be positive, whereas when the texture is primarily formed by dense tissue (*i.e.* the

gray-level histogram is skewed to lower values) the skewness values tend to be negative. Skewness is the third statistical moment, computed as:

$$skewness = \frac{w_3}{w_2^{3/2}}, \text{ where } w_k = \frac{\sum_{i=0}^{g_{max}} n_i (i - \bar{i})^k}{N}, \quad N = \sum_{i=0}^{g_{max}} n_i, \quad \bar{i} = \frac{\sum_{i=0}^{g_{max}} (in_i / N)},$$

and n_i represents the number of times that gray level value i takes place in the image region, g_{max} is the maximum gray-level value and N is the total number of image pixels.

Coarseness is a texture feature that reflects the local variation in image intensity; small coarseness value for an ROI indicates fine texture, where the gray levels of neighboring pixels are different; high coarseness value indicates coarse texture, where neighboring pixels have similar gray level values. Coarseness computation is based on the Neighborhood Gray Tone Difference Matrix (NGTDM) [2] of the gray-level values.

$$coarseness = \left(\sum_{i=0}^{g_{max}} p_i v(i) \right)^{-1}, \text{ where } v(i) = \begin{cases} \sum |i - \bar{L}_i| \text{ for } i \in \{n_i\} \text{ if } n_i \neq 0 \\ 0 \text{ otherwise} \end{cases}$$

is the NGTDM. In the above formulas, g_{max} is the maximum gray-level value, p_i is the probability that gray level i occurs, $\{n_i\}$ is the set of pixels having gray level value equal to i , and \bar{L}_i is given by ,

$$\bar{L}_i = \frac{1}{S-1} \sum_{k=-l}^l \sum_{l=-l}^l j(x+k, y+l)$$

where $j(x,y)$ is the pixel located at (x,y) with gray level value i , $(k,l) \neq (0,0)$ and $S=(2d + 1)^2$ with d specifying the neighborhood size around the pixel located at (x,y) .

Contrast and Energy, as defined by Haralick [2, 10], requires the computation of a gray-level co-occurrence matrix, based on the frequency of the spatial co-occurrence of gray-level intensities. Contrast quantifies the variation in image intensity, and energy is a measure of image homogeneity.

$$contrast = \sum_i \sum_j |i - j|^2 C(i, j), \text{ and } energy = \sum_i \sum_j C(i, j)$$

where g is the total number of different gray levels and C is the co-occurrence matrix[10].

One-way Analysis of Variance (ANOVA) was performed to estimate differences in the means of the texture feature distributions computed for different combinations of angular range and number of source projections. The average Pearson correlation coefficient (r) was also estimated between the texture features computed for the different DBT geometry acquisition settings.

3 Results

For all texture descriptors, the range of the computed features was affected by the DBT acquisition geometry. As shown for representative geometry settings (Fig. 3-4),

when keeping the angular range fixed and increasing the number of projections, skewness demonstrated a large increase ($p < 0.001$); coarseness and contrast a large decrease ($p < 0.001$); and energy a small increase ($p = 0.01$). When keeping the number of projections fixed and increasing the angular range, coarseness appeared to decrease ($p < 0.001$); contrast to increase ($p < 0.001$); and skewness and energy did not demonstrate significant variation ($p > 0.01$). For all texture descriptors, angular range appeared to have a greater effect on the correlation between the computed texture features, than the selected number of source projections. The correlation r was consistently stronger between features computed with the same angular range and different number of source projection images, rather than same number of source projections for different angular range (Fig. 3-4).

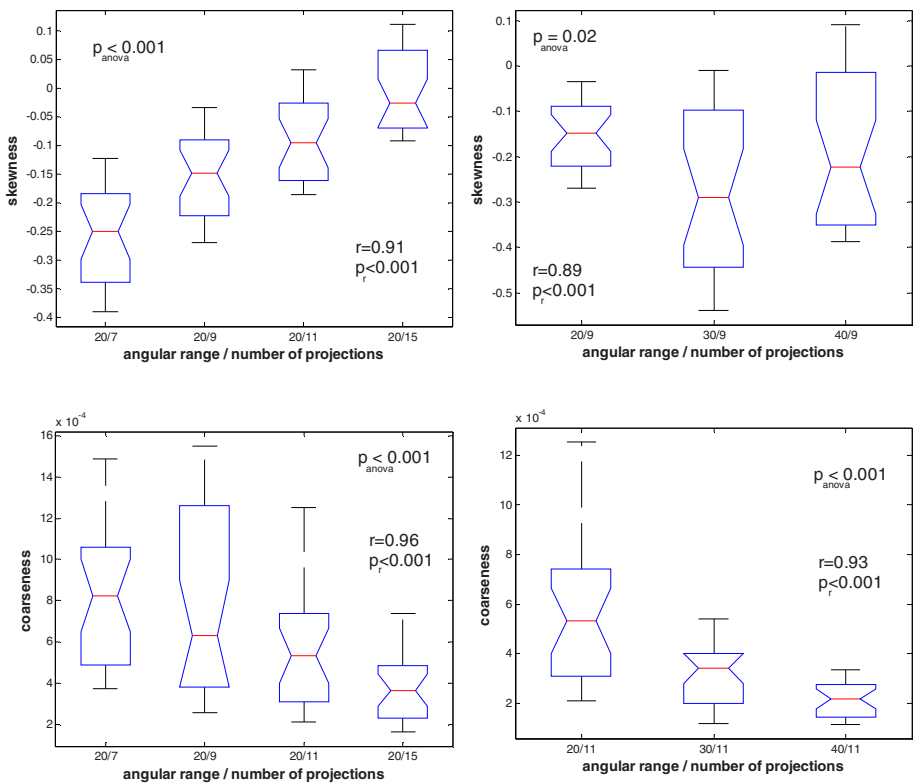


Fig. 3. Box-plots of the texture features f for skewness (up) and coarseness (down) having fixed angular range while varying the number of source projections (left) and for different angular ranges while acquiring the same number of source projections (right). The p -value of the ANOVA is shown, as well as the average Pearson correlation coefficient (r) with the associated p -value (p_r).

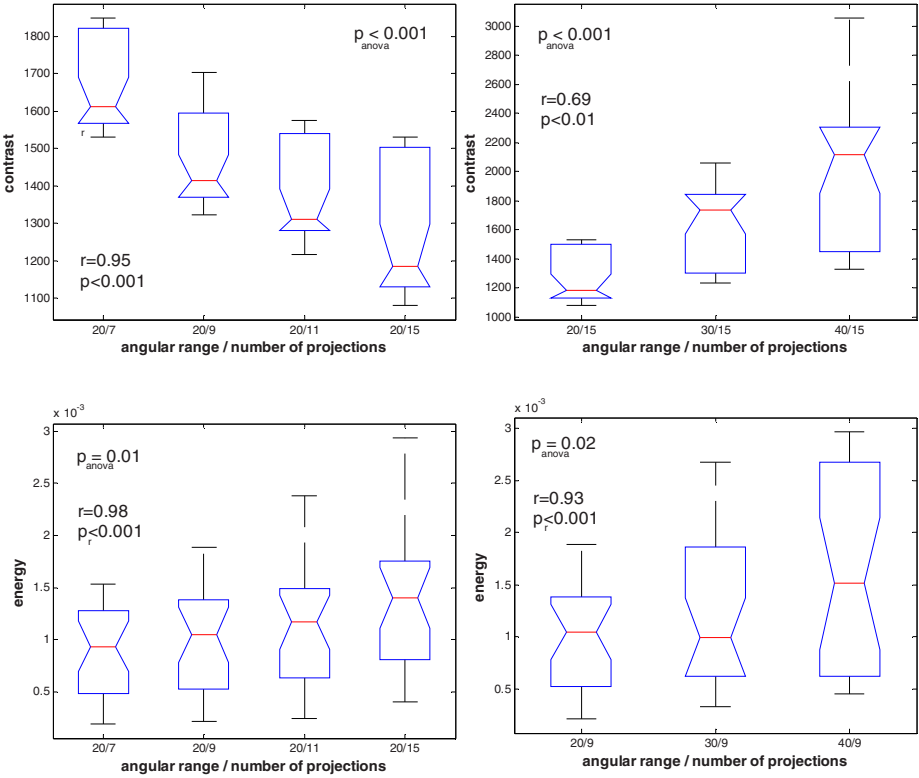


Fig. 4. Box-plots of the texture features f for contrast (up) and energy (down) having fixed angular range while varying the number of source projections (left) and for different angular ranges while acquiring the same number of source projections (right). The p -value of the ANOVA is shown, as well as the average Pearson correlation coefficient (r) with the associated p -value (p_r).

4 Discussion

We attribute the observed differences in the texture feature distributions to the effect of differences in image quality resulting from the different reconstruction geometries. As shown previously by Maidment *et al.* [6], both the use of increasing number of source projections for a fixed angular range, and the use of a larger angular range for the x-ray tube rotation, can improve DBT image quality. This effect can also be observed in our simulated DBT images (Fig. 5). By increasing the number of source projections, the reconstruction artifacts become less apparent; by increasing the angular range, the out of focus structures become more blurred, while the in-focus structures become more sharply defined. Although more clearly visible in real clinical data [6], these effects are also apparent in our simulated DBT images (Fig. 5).

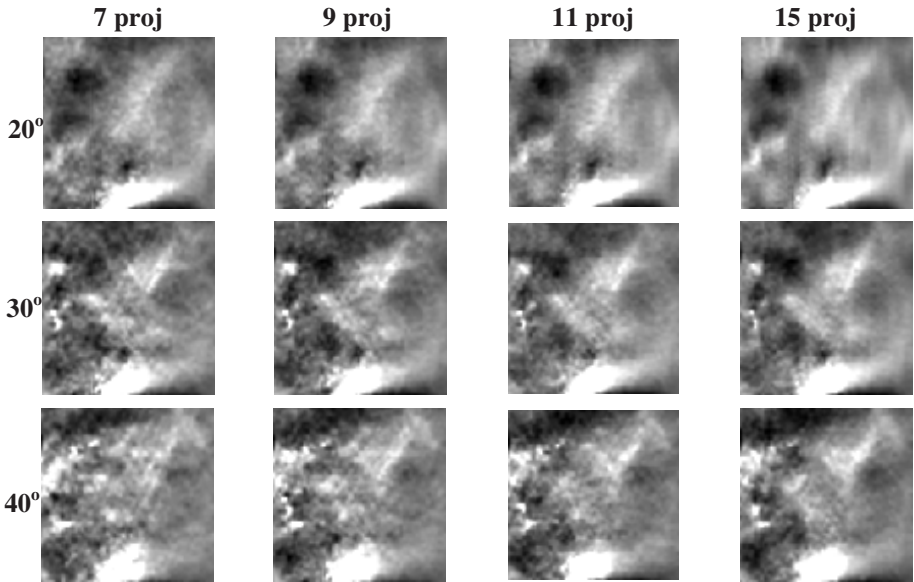


Fig. 5. Central tomographic slice from the synthetic DBT ROIs reconstructed from different simulated acquisition geometries: each row represents a fixed angular range (20°, 30°, and 40°) with the number of source projection images increasing from left to right (7, 9, 11, and 15)

As the reconstruction artifacts decrease with increasing numbers of projections, the image quality improves, potentially resulting in images with less skewed gray-level distributions (*i.e.* skewness values closer to zero), finer texture (*i.e.* lower coarseness values), and reduced gray-level variation due to the absence of artifacts (*i.e.* lower contrast). As the in-focus structures become better defined with increasing angular range, the image texture becomes finer (*i.e.* lower coarseness values) and the object structure becomes sharper (*i.e.* higher contrast). Note, however, that increasing the number of source projections, while keeping the angular range fixed, does not alter the out-of-plane blurring; it is only the variation of the angular range that directly affects the blurring of the out-of-focus structures [6]. Our results demonstrate this effect; texture features computed for the same angular range, with increasing number of projections, are consistently more highly correlated, compared to features computed with increasing angular range.

To the best of our knowledge, this is the first study to investigate the effect of DBT acquisition geometry on parenchymal texture. Our results show that DBT acquisition geometry can potentially have an effect on the estimated parenchymal texture features. Further analysis is underway to fully quantify this association using a broader range of DBT acquisition parameters and real clinical datasets. Our ultimate goal is to determine the DBT reconstruction geometry that provides the optimal image quality for estimating parenchymal texture features. The improved performance and relatively low cost of DBT will likely fuel the rapid and broad dissemination of DBT as a breast cancer screening modality; this will spur the development of DBT Computer-Aided Diagnosis (CAD) and Computer-Assisted Risk Estimation (CARE) systems in

clinical practice. Understanding the effect of DBT acquisition parameters on image texture features would overall benefit the optimization and design of such systems.

Acknowledgements. This work was funded by the Radiological Society of North America (FBRS0601 and RF0707), by the Susan G. Komen Breast Cancer Foundation (BCRT133506) and by the NIH/NCI Program Project Grant P01-CA85484.

References

1. Boyd, N.F., Guo, H., Martin, L.J., Sun, L., Stone, J., Fishell, E., Jong, R.A., Hislop, G., Chiarelli, A., Minkin, S., Yaffe, M.J.: Mammographic density and the risk and detection of breast cancer. *New England Journal of Medicine* 356(3), 227–236 (2007)
2. Li, H., Giger, M.L., Olopade, O.I., Margolis, A., Lan, L., Chinander, M.R.: Computerized Texture Analysis of Mammographic Parenchymal Patterns of Digitized Mammograms. *Academic Radiology* 12, 863–873 (2005)
3. Rafferty, E.A.: Digital mammography: novel applications. *Radiologic Clinics of North America* 45(5), 831–843 (2007)
4. Kontos, D., Bakic, P.R., Maidment, A.D.A.: Texture in Digital Breast Tomosynthesis: A Comparison between Mammographic and Tomographic Characterization of Parenchymal Properties. In: Giger, M.L., Karssemeijer, N. (eds.) *In Proc. SPIE Medical Imaging: Computer Aided Diagnosis*, San Diego, CA, vol. 6915 (2008)
5. Kontos, D., Bakic, P.R., Troxel, A.B., Conant, E.F., Maidment, A.D.A.: Digital Breast Tomosynthesis Parenchymal Texture Analysis for Breast Cancer Risk Estimation: A Preliminary Study. In: Krupinski, E. (ed.) *In Proc. International Workshop on Digital Mammography (IWDM) 2008*, Tucson, AZ. LNCS. Springer, Heidelberg (2008)
6. Maidment, A.D.A., Albert, M., Thunberg, S., AdelÖw, L., Blom, O., Egerström, J., Eklund, M., Francke, T., Jordung, U., Kristoffersson, T., Lindman, K., Lindqvist, L., Marchal, D., Olla, H., Penton, E., Rantanen, J., Solokov, S., Ullberg, C., Weber, N.: Evaluation of a Photon-Counting Breast Tomosynthesis Imaging System. In: Flynn, M.J. (ed.) *Proc. SPIE, San Diego*, vol. 5745, pp. 572–582. SPIE, Bellingham (2005)
7. Bakic, P.R., Albert, M., Brzakovic, D., Maidment, A.D.A.: Mammogram synthesis using a 3D simulation. I. Breast tissue model and image acquisition simulation. *Medical Physics* 29(9), 2131–2139 (2002)
8. Zhang, C., Bakic, P.R., Maidment, A.D.A.: Development of an Anthropomorphic Breast Software Phantom Based on Region Growing Algorithm. In: *Proc. SPIE Medical Imaging 2008: Visualization, Image-guided Procedures, and Modeling*, San Diego, CA, vol. 6918 (2008)
9. Ruiter, N.V., Zhang, C., Bakic, P.R., Carton, A.K., Kuo, J., Maidment, A.D.A.: Simulation of tomosynthesis images based on an anthropomorphic breast tissue software phantom. In: *Proc. SPIE Medical Imaging 2008*, San Diego, CA, vol. 6918 (2008)
10. Haralick, R.M., Shanmugam, K., Dinstein, I.: Textural features for image classification. *IEEE Transactions on Systems, Man and Cybernetics* 3, 610–621 (1973)